JOURNAL OF MATERIALS SCIENCE **36** (2001) 3657–3665

Valence compensated perovskite oxide system $Ca_{1-x}La_xTi_{1-x}Cr_xO_3$

Part III *Impedance spectroscopy*

R. K. DWIVEDI
School of Materials Science and Technology, Institute of Technology, Banaras Hindu University, Varanasi 221 005, India

D. KUMAR, O. PARKASH*
Department of Ceramic Engineering, Institute of Technology, Banaras Hindu University, Varanasi 221 005, India
E-mail: oparkash@banaras.ernet.in

Electrical behaviour of the compositions with $x \leq 0.50$ in the $Ca_{1-x}La_xTi_{1-x}Cr_xO_3$ system has been studied by employing complex plane impedance and spectroscopic analysis in the temperature range 100 K–550 K. These studies have revealed the contribution of three processes to the total electrical conductivity of these samples. An equivalent electrical circuit model, which contains series arrangement of three paralle RC elements, is proposed to represent the electrical characteristics of these materials. Out of these three, two processes correspond to the activated hopping processes within the bulk while the third process corresponds to the barrier layer formation in these ceramics. Immittance spectroscopic analysis shows that conduction occurs through localized as well as long range movement of charge carriers.

1. Introduction

In the past one and half decade we have been studying valence compensated perovskite oxide systems $M_{1-x}La_xTi_{1-x}M'_xO_3$ in details where M = Ba, Sr, Ca and M′ = Co, Ni, Fe [1, 2]. Lanthanum and cobalt doped strontium titanate ($Sr_{1-x}La_xTi_{1-x}Co_xO_3$) system exhibits relaxor like behaviour in the composition range $0.20 \leq x \leq 0.40$ [3]. Similar behaviour is exhibited by a few compositions in the system $Sr_{1-x}La_xTi_{1-x}Fe_xO_3$. In view of the interesting and useful properties exhibited by the above systems, it was considered worthwhile to investigate the possibility of formation an analogous system $Ca_{1-x}La_xTi_{1-x}Cr_xO_3$ and study its electrical properties in detail. Structure, dielectric behaviour and electrical charge transport behaviour of the system $Ca_{1-x}La_xTi_{1-x}Cr_xO_3$ have been communicated [4, 5]. The conductivity behaviour has been studied in the temperature range 300 K–1000 K. Measurement of DC conductivity below room temperature poses problem due to high electrical resistance of these materials. Further in order to understand the dielectric/electrical behaviour of these polycrystalline ceramic materials, it is necessary to separate the various contributions to the overall electrical behaviour. For this purpose, in this paper we are reporting the results of immittance complex plane and spectroscopic analysis on various compositions in the system $Ca_{1-x}La_xTi_{1-x}Cr_xO_3 (x \leq 0.50)$.

Electrical properties of electronic ceramics are result of different contributions from various components and processes present in the materials. In general, the overall dielectric properties arise due to inter-grain, intragrain and electrode processes. The motion of charge could take place in any fashion viz. charge displacement, dipole reorientation and space charge formation etc. [6, 7]. In order to achieve reproducibility and to have a control over the properties these, so called grains, grain boundaries and electrode contributions must be separated out. The method of complex impedance analysis [6, 7] has emerged as a very powerful tool for separating out these contributions. It is useful in studying defects, microstructures, surface chemistry and electrical conductivity for materials including dielectrics, ionic conductors, and adsorbate-adsorbent interfaces [8]. A brief account of complex immittance spectroscopic analysis is presented here.

AC response of a material can be expressed in any of the four basic formalisms. These are conventionally expressed as complex impedance (Z^*), admittance (Y^*), electric modulus (M^*) and permittivity (ε^*). These four functions are jointly called as 'Immittance functions. These are given as:

$$Z^* = Z' - jZ'' \quad (1)$$

$$Y^* = Y' + jY'' \quad (2)$$

*Author to whom all correspondence should be addressed.

$$M^* = M' + jM'' \tag{3}$$

$$\varepsilon^* = \varepsilon' - j\varepsilon'' \tag{4}$$

where

$$\tan\delta = \frac{\varepsilon''}{\varepsilon'} = \frac{M''}{M'} = \frac{Z'}{Z''} = \frac{Y''}{Y'} \tag{5}$$

and,

$$Z^* = \frac{1}{Y^*} = \frac{1}{\tau\omega\varepsilon_0\varepsilon_r}, M^* = \frac{1}{\varepsilon^*} \tag{6}$$

where $\omega(=2\pi f)$ is the angular frequency. $j = \sqrt{-1}$ and C_o is the capacitance of the empty cell i.e. geometrical capacitance.

The study of ε^* as a function of frequency has been widely used since the pioneering work of Cole and Cole [9]. It is most suited for dielectric materials having very low conductivity [6, 7]. For other type of materials, Z^*, Y^* and M^* are more suitable as they facilitate the modeling of equivalent circuits and easy visualization of various charge transfer process. It must be noted that Z^* and Y^* are inversely related. Hence, the frequency regions where response of materials under test is not visible in the Z^* plots would be highlighted in M^* plots. An 'RC' circuit has one time constant. It, therefore, can be conveniently used to represent one relaxation process.

Total impedance Z^* for the circuit containing one parallel RC component is given by:

$$Z^* = \frac{1}{j\omega C + 1/R} = \frac{R}{1 + j\omega CR} = Z' - jZ'' \tag{8}$$

where

$$Z' = \frac{R}{1 + \omega^2 C^2 R^2} \tag{9}$$

$$Z'' = \frac{\omega C R^2}{1 + \omega^2 C^2 R^2} \tag{10}$$

We get the relation between Z' and Z'' by eliminating ω

$$\left(Z' - \frac{R}{2}\right)^2 + (Z'' - 0)^2 = \left(\frac{R}{2}\right)^2 \tag{11}$$

This represent the equation of a circle with center co-ordinate (R/2,0) and radius equal to R/2, which passes through origin with its center on the real axis. The co-ordinate at the top of the semi-circular arc, at a particular frequency ω_o, is (R/2, R/2). Thus substituting $Z' = R/2$ and $Z'' = R/2$ in Equations 9 and 10, the relation $\omega_o RC = 1$ is obtained, where $\omega_o = 2\pi f_o$. The RC product is known as time constant i.e. relaxation time, τ. It should be noted that real and imaginary parts of these functions, referred as immittance functions, are always positive for dielectric or conductive materials [10]. Thus for single crystal only one semi-circular arc is obtained with single time constant. For a polycrystalline dielectric material, more than one semi-circular arc or depressed circular arcs may be obtained

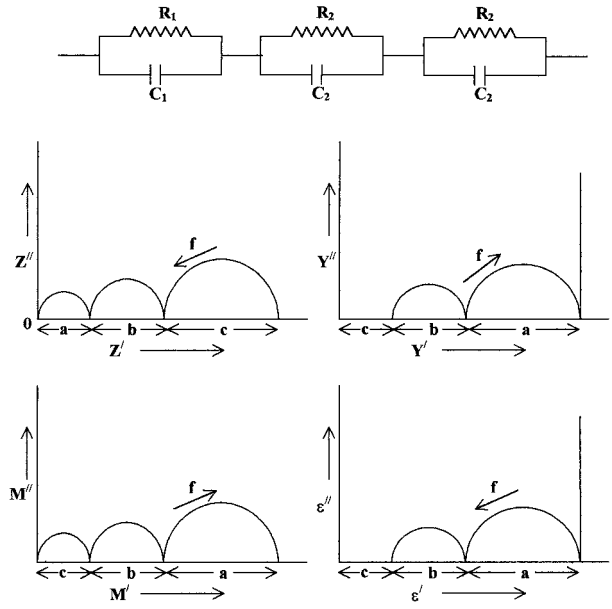

Figure 1 Equivalent circuit for a polycrystalline ceramic sample and corresponding frequency response in complex plane plots for four electrical formalisms.

depending on the number of processes having different time constants, τ's, such as τ_1, τ_2 and τ_3 [11]. The different time constants refer to the different RC products i.e. R_1C_1, R_2C_2 and R_3C_3 (Fig. 1). The different values of time constant correspond to different relaxation processes, occurring in various regions of polycrystalline materials. For example the conductivity of grains and grain-boundaries may be due to different processes and hence they relax in different frequency regions. In such type of materials, the equivalent circuit can be represented as a series network of parallel RC's elements [12] as shown in Fig. 1 and the impedance in this can be represented as

$$Z^* = \left[R_1^{-1} + j\omega C_1\right]^{-1} + \left[R_2^{-1} + j\omega C_2\right]^{-1} + \left[R_3^{-1} + j\omega C_3\right]^{-1} \tag{12}$$

where subscript 1, 2 and 3 represent the number of time constants.

In the impedance and modulus spectroscopic plots the imaginary part of impedance, Z'' and modulus, M'' are plotted as a function of frequency. In the spectroscopic plots, each relaxation process manifests itself in the form of a Debye type peak if the relaxation times for the different processes occurring in the material under ac field are separated from each other. The relaxation time is defined as the inverse of angular frequency at the maximum of the imaginary part of particular immittance function. For instance, τ_M denotes the modulus relaxation time at which M'' reaches the maximum, then $\omega\tau_M = 1$. Similarly τ_Z, τ_Y and τ_ε are relaxation times at which Z'', Y'' and ε'' exhibit maxima. If full width at half maximum (FWHM) is equal to 1.14 decade, then the peak is said to be an ideal Debye peak (i.e. having only one relaxation time) and if it is more than 1.14 decades, the relaxation times for different processes are comparable. The corresponding peaks overlap each

other to give a summation of Debye type peaks and it indicates that either there is a distribution of relaxation times or there is more than one relaxation process involved [11, 13]. The peak heights of Z'' vs log f and M'' vs log f are proportional to R_p and $1/C_p$ as given by the equations:

$$Z'' = \frac{R_p}{2} \tag{13}$$

$$M'' = \frac{C_0}{2C_p} \tag{14}$$

where C_o is the capacitance of the empty cell. Both impedance and modulus spectroscopic plots are complementary to each other. While the more resistive element dominates in the impedance spectrum, the less reactive or capacitive element dominates in the modulus spectrum.

A particular physical process can be represented by several relaxation times, depending on which dielectric function is chosen. The value of relaxation ratio, $\gamma = \varepsilon_S/\varepsilon_\infty$ where ε_S and ε_∞ represent the static dielectric constant and dielectric constant at very high frequency respectively, play very important role in determining the value of the relaxation time for a particular dielectric function. It, therefore, determines at what frequency the imaginary part of a particular dielectric function will have a peak ($\because \omega\tau = 1$) [14]. For a single relaxation process, it is found that ε'', Y'', Z'' and M'' peak at increasing frequency, i.e. $\tau_{\varepsilon''} > \tau_{Y''} > \tau_{Z''}\tau_{M''}$. With increasing value of relaxation ratio, the separation between these relaxation times increases. The frequency dependence of these dielectric functions can be expressed as

$$Z^* = \frac{1}{j\omega C_0 \varepsilon^*} \tag{15}$$

$$M^* = j\omega C_0 Z^* \tag{16}$$

It is advantageous to plot Z'' and M'' vs log f simultaneously (in the same graph). This helps in distinguishing whether a particular relaxation process in the material is due to short-range movement of charge carriers or due to long range movement of charge carriers [10]. But localized and long-range movement processes both may be the bulk processes. If the process is long-range then peak in M'' vs log f and Z'' vs log f will occur at the same frequency even for large relaxation ratios. If the process is localized, then these peaks will occur at different frequencies. This argument holds good for a single polarization process or processes having widely different time constant [14].

2. Experimental

The detailed method of preparation of various compositions in the system $Ca_{1-x}La_xTI_{1-x}Cr_xO_x (x \leq 0.50)$ by solid state ceramic method has been reported in part I of this series [4]. Sintered pellets were polished and coated with Ag-Pd paint, which is matured after firing at 800°C for 20 minutes. Capacitance, dissipation factor and conductance were measured as a function of frequency in the temperature range 100–550 K at different steady temperatures using HP – 4192 LF A impedance analyzer. Measurements were made during heating and cooling to check the reproducibility of the results on two pellets of each sample.

3. Result and discussion

Plots of Z'' vs Z' for all the compositions upto $x \leq 0.50$ are plotted at several steady temperatures. Typical complex plane impedance plots for the compositions with $x = 0.10$ and 0.30 at a few temperatures are shown in Figs 2 and 3 respectively. For $x = 0.10$, two clear circular arcs are observed at all temperatures. Plots of Z'' vs Z' for composition with $x = 0.05$ and 0.20 show similar behaviour. For $x = 0.30$, at low temperature i.e. 150 K one circular arc appears in the higher frequency range with a spike in low frequency range in its Z'' vs Z' plots. With increasing temperature, this spike in the low frequency range changes to another semicircular arc. At intermediate temperatures i.e. 300 K–400 K, two complete semicircular arcs are obtained. With further increasing temperature ($T > 400$ K), an arc lying in the high frequency range disappears while a new small arc begins to appear in the low frequency range. Similar results are obtained for $x = 0.50$.

Complex plane modulus plots for the representative samples with $x = 0.10$ and 0.30 are given in Figs 4 and 5

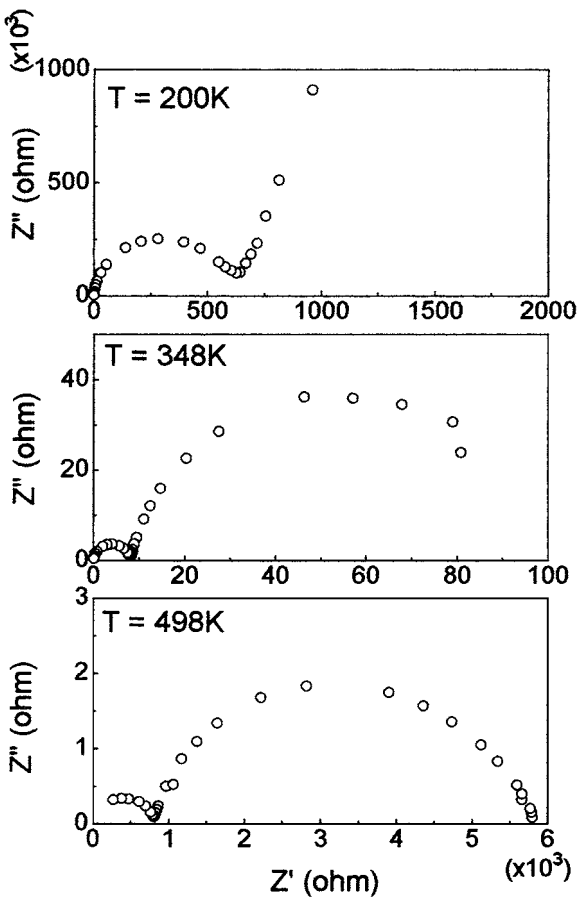

Figure 2 Plots of Z'' vs Z' at various steady temperatures for the composition $Ca_{0.90}La_{0.10}Ti_{0.90}Cr_{0.10}O_3$.

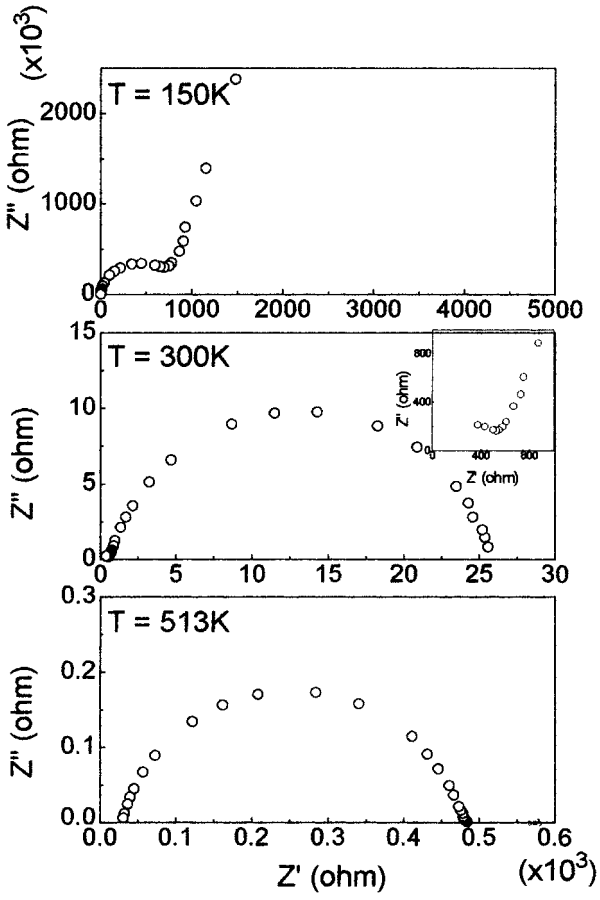

Figure 3 Plots of Z'' vs Z' at various steady temperatures for the composition $Ca_{0.70}La_{0.30}Ti_{0.70}Cr_{0.30}O_3$.

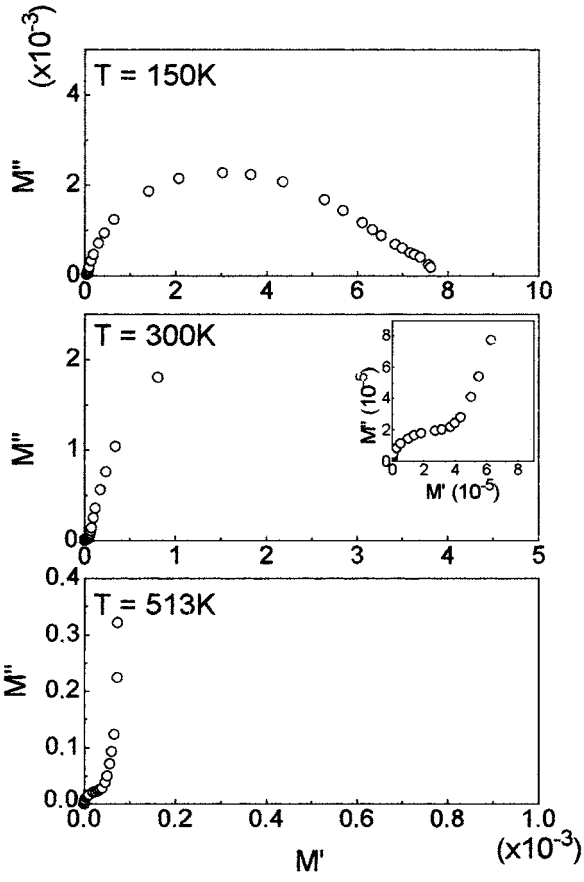

Figure 5 Plots of M'' vs M' at various steady temperatures for the composition $Ca_{0.70}La_{0.30}Ti_{0.70}Cr_{0.30}O_3$.

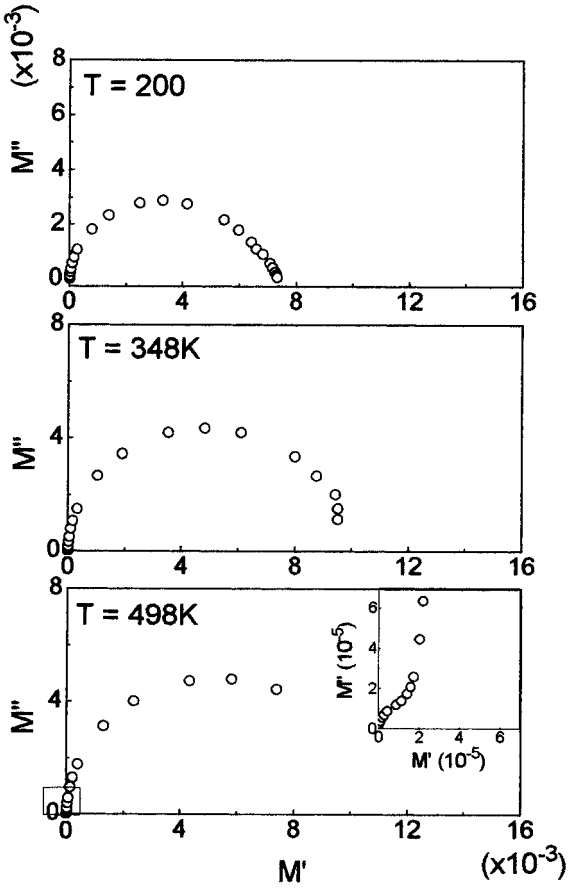

Figure 4 Plots of M'' vs M' at various steady temperatures for the composition $Ca_{0.90}La_{0.10}Ti_{0.90}Cr_{0.10}O_3$.

respectively at the same temperatures for which Z'' vs Z' plots are plotted. It is noted from these plots that for $x = 0.10$, two circular arcs are observed upto 200 K. With increasing temperature, the high frequency arc disappears while a low frequency arc passing through the origin, begins to appear. At ~500 K, again two circular arcs are obtained. Similar results are obtained for $x = 0.05$ and 0.20. For composition $x = 0.30$, two circular arcs are obtained upto ~300 K. At higher temperatures (i.e. at $T > 300$ K), the data points move towards low frequency arc which passes through the origin with a spike in the high frequency range. Similar results are obtained for $x = 0.50$ sample.

Values of C_1, C_2, C_3 for $x = 0.05$, 0.10 and 0.20 are obtained from the intercept of arcs in the complex plane modulus plots. The corresponding values of R_1, R_2 and R_3 are obtained from the highest point in these arcs where the relation $2\pi fRC = 1$ is satisfied, where f is the frequency of highest point. For $x = 0.30$ and 0.50, R_1, R_2 and R_3, and C_1, C_2 and C_3 were obtained from the complex plane impedance plots for $T \leq 300$ K. At higher temperatures the resistance and capacitance contributions were determined from Z'' vs Z' plots. These values are given in Table I. Plots of logarithms of resistance $R(R_1, R_2$ and $R_3)$ with inverse of temperature for these samples are shown in Fig. 6. Values of activation energy obtained from these plots for samples with x = 0.05, 0.10, 0.20 and 0.30 by least square fitting of the data, are given in Table II.

Z'' vs log f and M'' vs log f plots for all the compositions have been studied. For representative

TABLE I Values of resistance R_1, R_2, R_3 and corresponding capacitance C_1, C_2 and C_3 for various compositions (x) in the system $Ca_{1-x}La_xTi_{1-x}Cr_xO_3$

			$x = 0.05$			
Temp.→	100 K	200 K	313 K	397 K	485 K	529 K
R & C ↓						
R_1 (kΩ)	242	36.35	12.44	3.46	—	—
C_1 (nF)	0.66	0.44	0.26	0.23	—	—
R_2 (kΩ)	57680	2800	802.31	25.61	5.81	3.951
C_2 (pF)	92	114	66	62	55	56
R_3 (kΩ)	—	—	—	1160	525.30	389.30
C_3 (nF)	—	—	—	4.62	4.55	4.34
			$x = 0.10$			
Temp.→	200 K	313 K	348 K	395 K	450 K	498 K
R & C ↓						
R_1 (kΩ)	77.58	6.11	—	—	—	—
C_1 (nF)	0.29	0.26	—	—	—	—
R_2 (kΩ)	5702.10	455.82	66.67	3.51	1.179	0.627
C_2 (pF)	59	50	34	30	27	25
R_3 (kΩ)	—	90.90	53.578	28.58	19.658	15.31
C_3 (nF)	—	17.51	14.86	18.57	16.25	14.86
			$x = 0.20$			
Temp.→	100 K	150 K	200 K	300 K	380 K	480 K
R & C ↓						
R_1 (kΩ)	3642	691.90	73.30	2.07	0.52	0.11
C_1 (nF)	0.22	0.12	0.12	—	—	—
R_2 (kΩ)	21900	124.35	14.56	3.988	0.485	0.134
C_2 (pF)	38	44	55	57	66	24
R_3 (kΩ)	—	—	1138.3	1040.5	509.86	243.65
C_3 (nF)	—	—	27.99	2.15	1.56	1.18
			$x = 0.30$			
Temp.→	150 K	200 K	300 K	358 K	408 K	513 K
R & C ↓						
R_1 (kΩ)	175.64	83.018	6.124	—	—	—
C_1 (nF)	0.18	0.19	0.05	0.06	—	—
R_2 (kΩ)	1450.7	135.56	12.985	0.258	0.191	—
C_2 (pF)	55	59	61	88	84	—
R_3 (kΩ)	—	—	—	4.843	3.582	2.865
C_3 (nF)	—	—	—	6.59	6.35	7.94
			$x = 0.50$			
Temp.→	102 K	150 K	200 K	303 K	350 K	400 K
R & C ↓						
R_1 (kΩ)	15.546	3.185	2.654	1.185	0.201	0.055
C_1 (nF)	0.05	0.05	0.10	0.20	0.16	—
R_2 (kΩ)	23300	466.28	441.67	3.33	0.567	0.16
C_2 (pF)	68	68	181	2389	1080	996
R_3 (kΩ)	—	—	293	2.268	0.801	0.347
C_3 (nF)	—	—	27.22	70.55	6.64	4.69

TABLE II Values of activation energies, E_1, E_2 and E_3 for various compositions (x) in the system $Ca_{1-x}La_xTi_{1-x}Cr_xO_3$

	Activation energy					
	E_1(eV)		E_2(eV)		E_3(eV)	
Composition (x)	LT	HT	LT	HT	LT	HT
0.05	0.08	—	0.10	0.37	—	0.15
0.10	—	0.16	0.16	0.50	—	0.14
0.20	0.08	0.23	0.10	0.34	—	0.11
0.30	0.09	—	0.12	0.23	—	0.05
0.50	0.12	0.33	0.15	0.31	—	0.42

compositions with $x = 0.10$ and 0.30, these are shown in Figs 7 and 8. In these plots, as mentioned earlier, a peak appears corresponding to a particular polarization/relaxation process where the relation $2\pi fRC = 1$ is satisfied, where, R and C are the resistance and capacitance contribution of the RC circuit element corresponding to that process. Z'' vs log f plots highlight the circuit element, which is most resistive while M'' vs log f plots highlight the circuit element with least capacitance contribution. It is observed from Z'' vs log f plots for $x = 0.10$, that one peak occurs for $T \leq 313$ K. At $T \geq 397$ K, two peaks are observed, one in the low frequency range and another one in the high frequency range. The height of low frequency peak is higher than

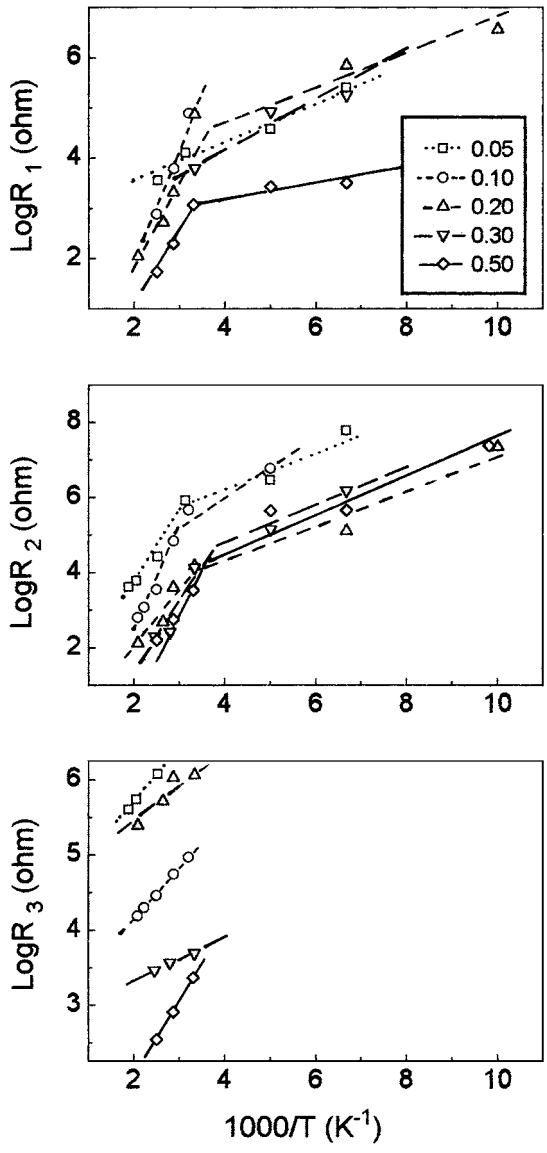

Figure 6 Variation of log $R(R_1, R_2$ and $R_3)$ with inverse of temperature for various compositions in the $Ca_{1-x}La_xTi_{1-x}Cr_xO_3$ system.

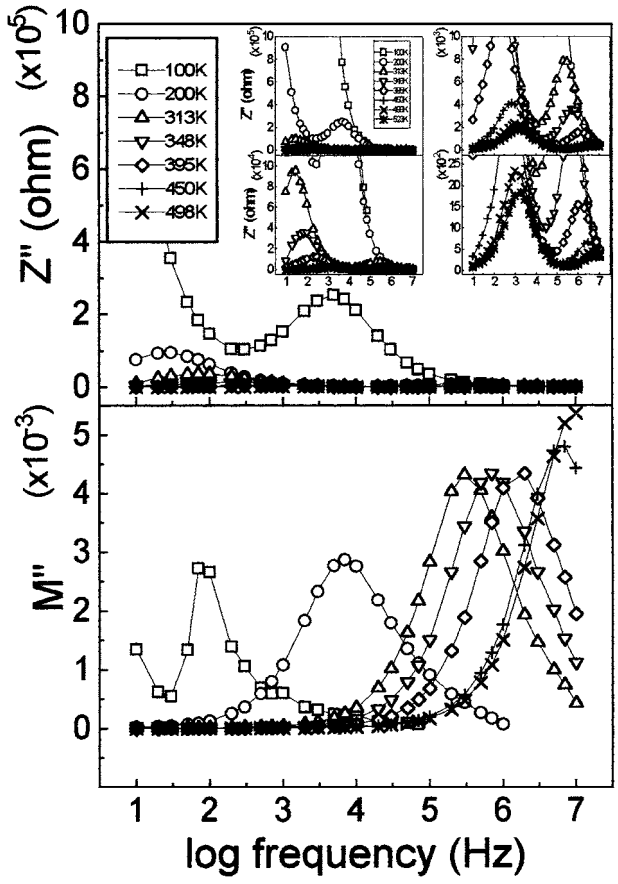

Figure 7 Variation of (a) Z'' and (b) M'' with log frequency at a few steady temperatures for the composition $Ca_{0.90}La_{0.10}Ti_{0.90}Cr_{0.10}O_3$.

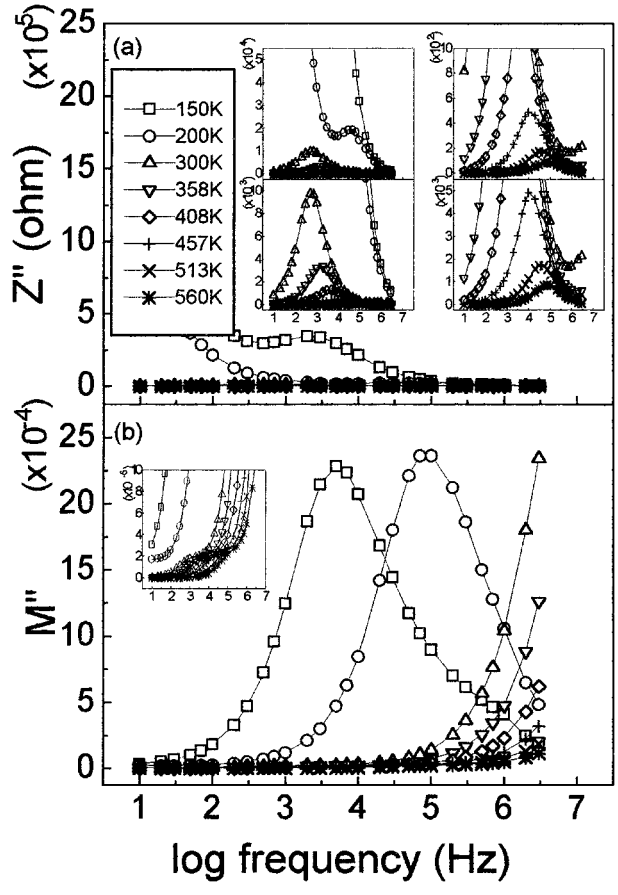

Figure 8 Variation of (a) Z'' and (b) M'' with log frequency at a few steady temperatures for the composition $Ca_{0.70}La_{0.30}Ti_{0.70}Cr_{0.30}O_3$.

that of high frequency peak. Full width at half maxima is in the range 1.40–1.65 at different temperatures. The high frequency peak position in Z'' vs log f plots almost coincides with the peak position in M'' vs log f plots. No peak, corresponding to low frequency peak observed in Z'' vs log f plots, is seen in the M'' vs log f plots. Behavior of the compositions with $x = 0.05$ and 0.20 is similar except that two peaks start appearing in the impedance spectroscopic plots for $T \geq 313$ K. Modulus spectroscopic plots exhibit a peak for $x \leq 0.20$. The frequency corresponding to a particular relaxation moves to higher side with increasing temperature. For $x = 0.30$, modulus spectroscopic plots show one peak at low temperature. At high temperature ($T \geq 300$ K) shoulder appears at low frequency side and high frequency peaks seems to shift beyond the measured frequency range. For $x = 0.50$, the modulus spectroscopic plots show two peaks for $T \leq 150$ K and one peak at $T \geq 200$ K. No peak is observed in the frequency range of measurement at higher temperatures for the samples with $x \geq 0.10$. The temperature range in which these peaks appear is different for different samples.

From the combined studies of complex plane immittance analysis (Z'' vs Z' and M'' vs M') and immittance spectroscopic analysis it is concluded that there are three polarization processes present in these materials. One, two or three of these processes are observed in a given formalism depending on the temperature and the composition.

The spectroscopic plots of Z'' and M'' at 400 K are shown in Fig. 9. It has been observed that for $x = 0.05$, M'' shows a peak in the range 100 kHz to 1 MHz whose full width at half maximum is 1.41 decades which is larger than an ideal Debye peak having FWHM of 1.14 decades. A careful examination of Z'' vs log f plot in the same figure shows a very small hump in the same frequency range. This hump in Z'' for $x = 0.10$, becomes larger and its peak frequency almost coincides with that of M'' peak. Besides this Z'' shows one more peak at lower frequency whose height is more as compared to the small hump at higher frequency. For $x = 0.20$, height of the low frequency peak in Z'' vs log f plots remains similar to $x = 0.10$ but a small hump appears in M'' vs log f whose frequency coincides with the peak frequency in Z''. The high frequency peaks in Z'' and M'' (corresponding to high frequency peak in $x = 0.10$) seems to be shifted beyond the range of frequency measurement. For $x = 0.30$, the peak in Z'' vs log f plots shifts to higher frequency side as compared to $x = 0.20$ while no peak is observed in M'' in the frequency range of measurement. There may be a peak at higher frequencies. Similar results are obtained for $x = 0.50$.

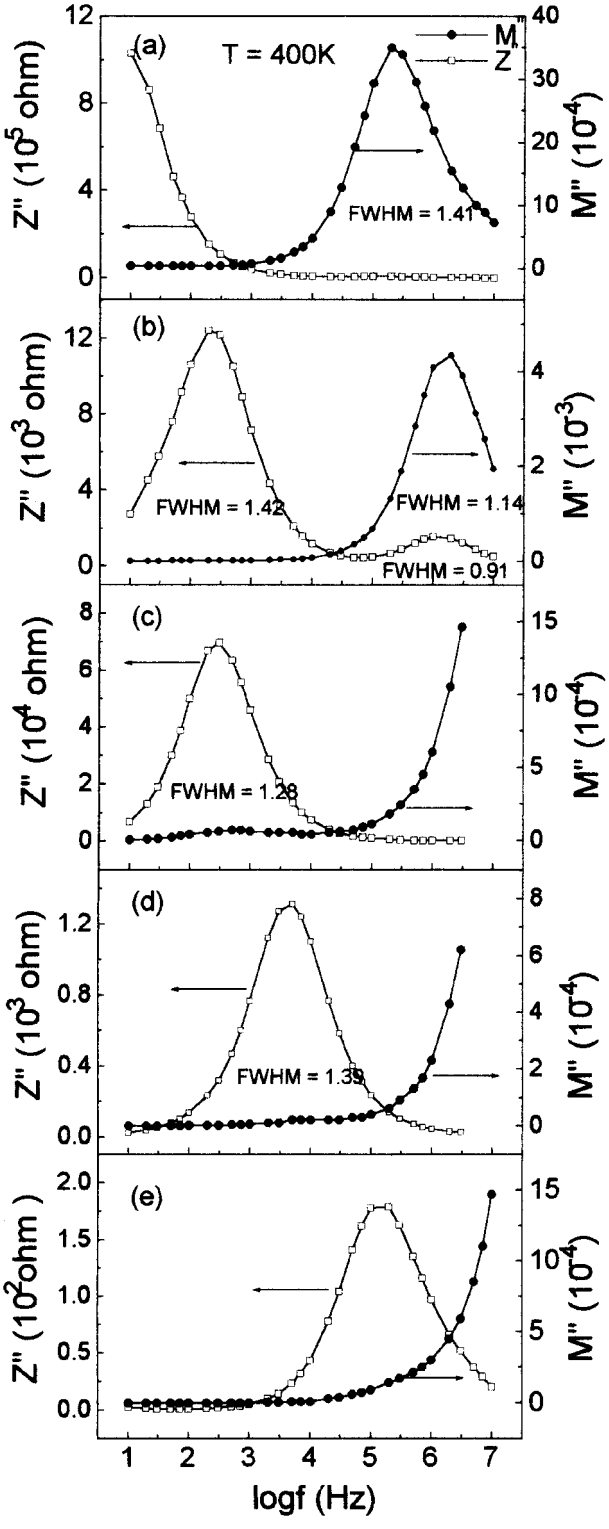

Figure 9 Impedance and modulus relaxation spectroscopy plots at 400 K for various compositions x (a) 0.05, (b) 0.10, (c) 0.20, (d) 0.30 and (e) 0.50 in the system $Ca_{1-x}La_xTi_{1-x}Cr_xO_3$.

It has been reported that electrical conduction behaviour of different compositions in this valence compensated system are dominated by acceptor chromium Cr^{3+} ions [5]. The ac electrical characteristics ($\log \sigma_{ac}$ vs log f plots) of these compositions are similar to the acceptor doped titanates having high insulation resistance because grain boundaries act as a highly resistive barriers for cross transport of charge carriers [15]. The grain boundary barriers are caused by grain boundary states that are oppositely charged as compared to the background dopant centres in the bulk. This causes a depletion of mobile carriers in the vicinity of grain boundaries. The grain boundary depletion space charge layers are described as back to back double Schottky barriers. The width of the grain boundary space charge layer depends on the acceptor concentration, the temperature and oxygen partial pressure during firing. Vollmann and Waser [16] represented the ceramic samples by brick wall model. In this model, the ceramic corresponds to an electrical network consisting of two parallel R-C circuits connected in series. One of these RC element corresponds to the bulk and the other to the grain boundaries contribution. For such an equivalent circuit, representing the ceramics, two plateaus are observed in $\log \sigma_{ac}$ vs log f plots. The plateau in the low frequency range gives the total conductivity of the sample while the high frequency plateau gives the bulk conductance. The two plateaus are separated by a frequency dependence region having a slope 1 [15].

It is noticed from the Table II, that activation energy for grains (E_1) and grain boundaries (E_2) in the low temperature regime ($T < 250$ K) are almost same i.e. around 0.10 eV for all these samples. In the high temperature regimes ($T > 250$ K), there is a significant difference in the E_1 and E_2 for $x = 0.05$, 0.10 and 0.20. The values of E_2 is higher than E_1. This can be ascribed to increased disorder present in the grain boundaries which leads to more scattering of charge carriers. In the low temperature region conduction occurs due to thermal rotation of dipoles which do not involve long range movement of charge carriers as will be discussed later. Hence the activation energies for conduction are equal for grains and grain boundaries.

In the present system, two plateaus connected by a frequency dependent region (e.g. for $x = 0.10$ at $T \geq$ 300 K) or two frequency dependent regions connected by a plateau (for $x = 0.20$ at 150 K) or a single plateau and one frequency dependent region (e.g. for $x = 0.30$ at $T = 560$ K and for $x = 0.50$ at $T \geq$ 300 K) were observed [5]. All the three plateaus and frequency dependent regions could not be observed in any sample simultaneously at any temperature in the frequency range of measurement. This is due to limited temperature and frequency range available in the experiments. The high frequency plateau, observed at low temperatures is only observed in $x = 0.05$ and 0.10 for $T \leq$ 300 K. This gives the contribution of one bulk process, which does not relax in the highest frequency available at these temperatures. The low frequency plateau at low temperatures in these samples shifts to high frequency range at high temperatures in these and other samples and corresponds to the total conductivity of both the bulk processes. The low frequency plateau, appearing at $T \geq 300$ K in all the samples, corresponds to the total conductivity (including grains as well as grain boundaries).

It follows from the frequency dependence of AC conductivity [5], dielectric behavior [4] and complex plane immittance analysis that there are three contributions to the overall electrical/dielectric behavior. The contribution which appears in the high temperature ($T \geq 300$ K in all the samples) and low frequency region is due to interfacial space charge polarization present at grains – grain boundaries interfaces. Its time constant, RC is large due to large values of R and C (Table I). R decreases with increasing temperature and its contribution appears as a small arc in the low frequency region in the complex plane modulus plots. The capacitance associated with this contribution is in the nano-Farad range. This order of capacitance is assigned to thin regions like grain boundaries interfaces [13]. This contribution appears only above a certain temperature. This is because at lower temperatures, the dc conductivity due to long range movement of the charge carriers is small. It increases exponentially with temperatures. Therefore, with increasing temperature, these charge carriers can transport easily through the bulk, get intercepted at the grain-boundaries, which act as barriers for their cross transport. This trapping of charge carriers at grain-boundaries gives rise to space charge polarization. This is manifested by a rapid rise in dielectric constant with temperature in the high temperature range. This contribution of space charge polarization is clearly seen in ε_r vs log f plots of compositions with $x = 0.20$ and 0.30 in the intermediate frequency region [4]. The relaxation seems to be similar to the Debye relaxation process. The resistive part of this contribution can be obtained from the difference in the resistance corresponding to low frequency plateau and high frequency plateau observed in $\log \sigma_{ac}$ vs log f plots for all the compositions.

Immittance spectroscopic plots are useful to decide whether a particular relaxation process is due to long range or short range movement of the charge carriers. If different functions ε'', $\tan\delta$, Y'', Z'' and M'' are plotted as a function of frequency at a given temperature, then the relaxation time for a particular process, which is given by inverse of the angular frequency corresponding to the peak have increasing value in the order $\tau_\varepsilon \geq \tau_Y > \tau_{\tan\delta} > \tau_Z \geq \tau_M$ [14]. Further it can be shown that if a processes occurs due to long range movement of charge carriers, then τ_Z and τ_M will be equal. They will be different with $\tau_Z > \tau_M$ for the short range movement of charge carriers. The difference between τ_Z and τ_M becomes more significant with larger relaxation ratio, $\varepsilon_S/\varepsilon_\infty$

It is noted from the plots of Z'' and M'' vs log f for various compositions that there is only one peak in the M'' vs log f plot (Fig.9). There is a small hump in the Z'' vs log f plot whose frequency seems to coincide with the frequency of M'' peak in this plot for $x = 0.05$ in the observed frequency range. Two peaks in Z'' vs log f plot and one peak in M'' vs log f plot are observed for $x = 0.10$ (Fig. 9b). The high frequency peak in Z'' plot occurs at the same frequency where M'' peaks. For $x = 0.20$ and 0.30, only one peak is observed in M'' vs log f plots which seems to occur at the same frequency where a hump in Z'' vs log f appears.

These materials contain associated defect pairs $Cr_{Ti'}^{3+}$ - $V_0^{\bullet}$ - Cr_{Ti}^{4+} or $2Cr_{Ti'}^{3+}$ - $V_0^{\bullet\bullet}$ [5] where all the species are written in accordance with Kroger - Vink notation of defects [17]. These defect pairs from dipoles. These dipoles can change orientation due to hopping of holes among Cr^{3+} and Cr^{4+} sites. Beside this oxygen ions can jump through $V_0^{\bullet\bullet}$ sites around $TiO_5V_0^{\bullet\bullet}$ or $CrO_5V_0^{\bullet}$ or $CrO_5V_0^{\bullet\bullet}$ octahedra. This type of relaxation has been reported in a number of acceptor doped perovskites at low temperature [18]. At low temperatures, these processes give rise to two types of orientation polarization and localized conduction [4]. This explains equal values of activation energies obtained from dielectric relaxation and conductivity measurements. This process also accounts for the observed frequency dependence but weak temperature dependence of AC conductivity [5]. With increasing temperature, these dipoles get dissociated and long range movement due to hopping of charge carriers occurs. A higher activation energy in this temperature range includes dissociation energy of these dipoles. The charge carriers which undergo long range movement in grains, giving rise to DC conductivity, get intercepted at the grain boundaries. This gives rise to space charge polarization which is manifested as a rapid rise in dielectric constant at low frequencies at high temperatures [4].

The peaks in Z'' vs log f and M'' vs log f plots, which occur at the same frequency as mentioned above, correspond to long range movement of charge carriers. This may be due to hopping of holes among Cr^{3+} and Cr^{4+} sites. The relaxation frequency for $x = 0.20$ and 0.30 is less as compared to $x = 0.05$ and 0.10 for this process. The peaks corresponding to orientational polarization which involves short range movement of charge carriers may occur beyond the frequency range of measurements. There is no peak in M'' vs log f plot of $x = 0.10$ corresponding to low frequency peak in Z'' vs log f plot. One reason for this, as already mentioned, may be that the capacitance associated with this process is very large as compared to the capacitance corresponding to the high frequency process. This, therefore, gets suppressed in the modulus spectroscopic plots [13].

4. Conclusion

Immittance spectroscopy shows that there are three contributions to the observed polarization/conduction processes. These are two orientational polarization caused due to hopping of holes among defect complexes with in the bulk and one space charge polarization occurring at the interface. An equivalent circuit model of the electrical network in these materials is proposed to contain three parallel *RC* elements arranged in series. At low temperature conduction occurs among localized Cr^{3+} and Cr^{4+} sites which leads the reorientation of dipoles whereas at high temperature conduction occurs due to long range movement of charge carriers among these sites.

Acknowledgements

Financial support from Department of Science and Technology is gratefully acknowledged. One of the Authors Mr. R. K. Dwivedi is also thankful to DST for providing him financial assistance during the course of these investigations.

References

1. CH. D. PRASAD, Ph.D. Thesis, Banaras Hindu University, Varanasi, India, (1988).
2. C. C. CHRISTOPHER, Ph.D. Thesis, Banaras Hindu University, Varanasi, India (1988).
3. OM PARKASH, CH. DURGA PRASAD and D. KUMAR, *J. Mater. Sci.* **25** (1990) 487.
4. R. K. DWIVEDI, OM PARKASH and D. KUMAR, *ibid.* Part I, communicated.
5. *Idem.*, *ibid.* Part II, communicated.
6. A. R. VON HIPPEL, "Dielectrics and Waves" (John Wiley & Sons, London, 1995).
7. J. R. MACDONALD, "Impedance Spectroscopy" (John Wiley & Sons, New York, 1987).
8. L. L. HENCH, in Proc. 14th Symp. Soc. Arosp. Mater. Process Engg. (1968) P. 1.
9. K. S. COLE and R. H. COLE, *J. Chem. Phys.* **9** (1941) 341.
10. W. CAO and R. GERHARDT, *Solid State Ionics* **42** (1990) 213.
11. J. T. S. IRVINE, D. C. SINCLAIR and A. R. WEST, *Adv. Mater.* **2** (1990) 132.
12. R. GERHARDT and A. S. NOWICK, *J. Amer. Ceram. Soc.* **69** (1986) 641.
13. I. M. HODGE, M.D. INGRAM and A.R. WEST, *J. Electroanal. Chem.* **74** (1976) 125.
14. R. GERHARDT, *J. Phys. Chem. Solids* **55** (1994) 1491.
15. R. MOOS and K.H. HARDTL, *J. Amer Ceram Soc.* **80** (1997) 2549.
16. M. VOLLMANN and R. WASER, *ibid.* **77** (1994) 235.
17. F. A. KRÖGER and H. J. VINK, in "Solid State Physics," Vol 3, edited by F. Seitz and D. Turnbull, Academic Press, New York, 1956, p. 307.
18. A. S. NOWICK, S. Q. FU, W. K. LEE, B. S. LIM and SCHERBAN, *J. Mater. Sci. Engg.* **B23** (1994) 19.

Received 27 June 2000
and accepted 6 February 2001